American Journal of Nanomaterials, 2023, Vol. 11, No. 1, 61-71
Available online at http://pubs.sciepub.com/ajn/11/1/5
Published by Science and Education Publishing
DOI:10.12691/ajn-11-1-5

SciEP
sciepub.com

Review of Recent Advances of GaN Nanowires Based Sensors

H. Murad, W. Hashim, Ahmed M. Nahhas*

Department of Electrical Engineering, Faculty of Engineering and Islamic Architecture,
Umm Al Qura University, Makkah, Saudi Arabia
*Corresponding author: anahhas@hotmail.com

Received January 05, 2023; Revised February 11, 2023; Accepted February 20, 2023

Abstract This paper presents a review of the recent advances of GaN nanowire-based sensors. GaN nanostructures of various forms including nanowires, nanotubes, nanofibers, nanoparticles and nanonetworks have been reported for several sensing applications due to their unique electrical, optical, and structural properties. The nature of GaN materials provides advantages for nanodevices compared to thin films due to its higher surface-to-volume ratio. In addition, GaN materials can absorb ultraviolet radiation which is a key feature in several optical applications. These advantages led to much attention and further study in the applications of GaN. In this paper, the recent advances of GaN sensing applications such as gas sensors, biosensors, and pressure sensors are presented. The performance of these sensors is demonstrated along with the structural, electrical, and optical properties of GaN.

Keywords: *gallium nitride (GaN), nanostructured, doping, nanowires, sensors, ultraviolet (UV)*

Cite This Article: H. Murad, W. Hashim, and Ahmed M. Nahhas, "Review of Recent Advances of GaN Nanowires Based Sensors." *American Journal of Nanomaterials*, vol. 11, no. 1 (2023): 61-71. doi: 10.12691/ajn-11-1-5.

1. Introduction

Over the past two decades, three-dimensional gallium nitride (3D GaN) has been widely used in light-emitting diodes, sensors, laser diodes, solar cells, and power electronics [1], attributing to its excellent optical and electronic properties. In 2004, graphene was successfully exfoliated and proved to have extraordinary properties [1]. Inspired by graphene, theoretical calculations have proved that two-dimensional hexagonal GaN (2D h-GaN) is stable [1]. Zhang et al. predicted that h-GaN can be used as excellent electrode material in lithium-ion batteries [2]. The advantage with these materials is the flexible bandgap varying from 0.7 to 6 eV hence covering an ultra-broad spectrum, from deep ultraviolet up to near infrared [3,4], allowing the development of numerous applications [3,4]. Major efforts have been dedicated to the technological fabrication to achieve efficient emitters and detectors [3,4]. Recent progress has demonstrated cutting edge results in high-speed data rate connectivity and integrated circuits [3,4]. Imaging sensors on high-speed electronics have been implemented founded on their sensitive applications in security screening [3,4].

GaN as a member of group III-nitride family has become a revolutionary material owing to its electronic and optical properties [3,4]. The direct, flexible, and wide bandgap makes GaN materiel a key candidate for achieving high frequency, large bandwidth, high power, and efficiency devices [3,4].

GaN based detectors are suitable for full color display, high density information storage, and UV communication links [3,4].

GaN is a very hard, chemically, and mechanically stable wide bandgap (3.4 eV) semiconductor material with high heat capacity and thermal conductivity which makes it suitable to be used for sensors [9], for high power electronic devices such as field effect transistor (FET) [3,4] and for optoelectronic devices such as light emitting diode (LED) [3,4]. The optical properties of GaN nanostructured are of great current interest because of the potential application in solid state lighting [3,4]. In *n*-type GaN, a UV peak at approximately 3.42 eV usually dominates the photoluminescence spectrum [3,4]. The blue luminescence at 2.7 to 3 eV peak energy has been extensively studied; this peak dominates due to optically active defects and impurities [3,4]. On the other hand, such defects can be destructive in a device. A well-engineered inorganic nanoparticle approach offers many advantages [3,4]. Meanwhile, in nanostructures having a large specific area, the surface states effect became significant in influencing the carrier recombination mechanism [3,4].

The efficient *p*-type doping of GaN is in general a challenging task [3,4]. The magnesium (Mg) ion implantation for *p*-type conductivity is more challenging due to the higher temperature annealing required for electrical activation, resulting in a major difficulty protecting the surface [3,4]. Mg is the only dopant capable of ensuring stable, reproducible *p*-type conduction in GaN [3,4]. The formation energy of Mg on the Ga site (MgGa) near the valence band is about 1 eV higher than that of SiGa

at the Fermi level near the conduction band [3,4], which may explain the difference of required annealing temperature for different conduction types. The efficient *p*-type doping of GaN is in general a challenging task [3,4]. The extrinsic carbon doping delivers better dynamic properties for the device voltage capabilities. Carbon doping has been traditionally achieved through incorporation of carbon originating from the metal organic precursor during the growth process [3,4] in a so-called auto doping technique. GaN can also be doped with europium (Eu). It is an attractive alternative to InGaN for the red-light LED, as the InN rich alloy has disappointingly low luminescence efficiency [3,4]. GaN can also be doped with manganese (Mn). The growth of homogeneously Mn-doped Ga1_xMnxN thin films have been carried out at different temperatures [3,4]. A high dopant concentration and high carrier concentration are inherent advantages of that doping [3,4]. The Pulsed laser deposition (PLD) can be used to prepare thin films from multicomponent targets and allows Mn concentrations in the GaN films to be controlled easily by varying the quantity of Mn included in the initial target preparation [3,4]. The growth conditions can be far from equilibrium, which offers the possibility of reaching higher Mn concentrations without phase separation [3,4]. The study of nanostructured materials doping was reported and investigated by Nahhas [3]. In that work, GaN doping processes and the challenges of each process were presented and discussed [3]. GaN nanostructured material exhibits many advantages for nanodevices because of its higher surface-to-volume ratio as compared to thin films [3]. The GaN nanostructured material has the ability to absorb UV radiation and immense in many optical applications [3]. The electronic properties of quantum confinement of electrons of nanoparticles make them very useful in electronic industry including many GaN applications [3]. Nanomaterial based sensors for environmental monitoring exhibited excellent potential in detection of trace contaminants due to the unique features of nanomaterials such as strong adsorption capacity, high surface area and reactivity, and large catalytic efficiency [5,6,7].

The design of high-power GaN devices is strongly affected by the self-heating [8,9], and accurate thermal management is needed to control the temperature of such devices. Fourier's law describes heat diffusion when the characteristic length scale of thermal transport is much longer than the phonon means free path (MFP). However, if the size of a hotspot is small enough, it will induce nonlocal (also called quasi- ballistic) transport phenomena [10]. Then, non-diffusive thermal energy phonon carriers will travel from the source before experiencing collisions, and Fourier's law is no longer adequate to describe thermal transport at the nanoscale [10].

High-quality epitaxial GaN growth is now possible thanks to the native GaN substrates available in the market [11]. The only disadvantage of these freestanding GaN substrates is their high cost for commercial applications [11]. One efficient way to reduce the total process cost is to isolate the epitaxial device from the bulk GaN substrate and reuse it. Several lift-off methods such as growth over patterned masks, natural stress-induced separation, controlled spalling, chemical etching of sacrificial layers, substrate removal by grinding/ etching, the use of weakly bonded detach layers like graphene, and laser lift of are reported for separating GaN films from the foreign substrates [11,12]. Separating GaN film from a GaN substrate is also reported by using various techniques like chemical lift of process, creating porous release layers via chemical etching or dry etching, controlled spalling, laser lift-off with an InGaN sacrificial layer [11], and ion implantation [12].

2. GaN Nanostructured Materials Doping

GaN nanostructured have various shapes including nanowires, nanoparticles, nanobelts, nanorings, nanotubes [12], nanodots [13], and nanorods [14]. GaN nanoparticles generated lot of interest among scientists as well as technologists during past few years.

The ion implantation technique for controlling *n*-type or *p*-type conduction has been a significant challenge for GaN based high-power devices to achieve levels approaching their theoretical limits of performance [15]. Despite the achievements in realization of good quality *p*-type GaN, the activation efficiency of Mg atoms is still as low as few percent. The *p*-type doping of GaN is typically performed during growth, while the reports on other doping techniques common in semiconductor processing such as ion implantation [16].

Table 1. *n*-type nearest-neighbour bond length (NNBL in A) around substitute defect, Ga-N bond length (HBL in A) in perfect GaN, most stable charge state (MMCS), magnetic moment (MM in uB) [17]

n-type	MMCS	MM (μB)	NNBL (Å)			HBL (Å)
C_{Ga}	0	0	1.408	1.408	1.407	1.85
	1+	0	1.412	1.412	1.406	
Si_{Ga}	0	0	1.698	1.698	1.697	
	1+	0	1.695	1.695	1.693	
Ge_{Ga}	0	0	1.807	1.807	1.807	
	1+	0	1.796	1.796	1.795	
O_N	0	0	1.925	1.925	1.926	
	1+	0	1.932	1.932	1.933	
	0	0	2.211	2.211	2.216	
S_N	1+	0	2.208	2.208	2.215	
Se_N	0	0	2.294	2.294	2.301	
	1+	0	2.290	2.290	2.299	

There have been several advancements in GaN doping processes. This subject was reported and investigated by Liu et al. [17]. Their work systematically studied the structural, magnetic, and defect properties of 12 kinds of dopants in the two-dimensional hexagonal gallium nitride (2D h-GaN) system [17]. The results showed that the most stable charge states (MSCSs) for *n*-type systems are 0 and 1+, and all the *n*-type substitutes acted as shallow donors. The MSCSs of the *p*-type systems are 1+, 0 and 1+, and the acceptor ionization energy was distributed higher than the valence band maximum (VBM) from +1.25 to 2.85 eV, acting as deep acceptors, which would capture electrons (holes) in *n*-(*p*-type) 2 D h-GaN and act the carrier conductivity. Thus, it was difficult to achieve *p*-type doping through a single defect in 2D h-GaN, and complex defects were necessary to achieve *p*-type doping experimentally [17]. For *n*-type 2D h-GaN system,

nearest-neighbor bond length (NNBL in A) around the defect, Ga-N bond length (HBL in A) in host GaN, most stable charge state (MMCS) and magnetic moment (MM in B) are shown in Table 1 [17].

3. GaN Nanowires Sensors Based Devices

GaN Nanowires Sensors has potential applications in quantum communication, quantum cryptography and other single-photon sources [18]. In the present-day world, all types of biological and chemical process involved in agriculture, industrial-drugs, semiconductors, textiles, food, consumer goods, and healthcare depend on the right pH levels [19]. Numerous efforts have been made in the past towards device development of various pH sensors [20]. Supervision and control of the pH level is important for preventing unwanted chemical reactions and for optimizing desired reactions [20]. They include micro-cantilevers, ion sensitive field effect transistor (ISFET) technology, thin-film technology (TFT), glass membrane pH electrodes, fiber optic pH sensors, and potentiometric pH sensors [21,22]. Lately, the group III-V semiconductors based high electron mobility transistors (HEMTs) are being explored as suitable candidates for pH sensing. Properties of GaN material devices such as the wide band gap, compatibility with high-temperature environment, strong chemical stability and good biological suitability make them interesting sensor materials [20].

Because of biocompatibility and stable chemical properties, AlGaN and InGaN are also important candidates for performance enhancement of pH sensors. These materials also have large sheet carrier concentration, a wide band gap and a higher sensitivity for harsh environments like high temperature and acidic or alkaline solutions [20]. The quaternary compound InAlGaN was studied as a new barrier layer in the HEMTs to overcome the problems of lattice mismatch and immiscibility in the alloys [23,24]. A recent study reported by Upadhyay et al. [23,24]. aimed to provide an insight into the performance of the quaternary InAlGaN heterostructures, specifically as a pH sensor [20]. In their work, they explored the physical factors that control the performance and sensitivity of the InAlGaN-based sensors depending on their structural parameters [20]. They also compared various design parameters, changes in the threshold voltage, transconductance, and sensitivity of the InAlGaN/GaN and AlGaN/GaN materials systems [20]. In addition, they found an optimized In and Al mole fraction composition for the best pH specific sensitivity [20]. The results of their model at 0% In and 23% Al mole fractions, matched closely with the experimental data reported by Kokawa et al. [20] for AlGaN/GaN HEMT as shown in Figure 1. With the higher mole fraction of In, the threshold voltage of the devices shifted more towards the negative value [20]. They also noticed that there is a change in the threshold voltage when the gate area of the device is exposed to air and when the electrolyte solution with certain pH value is filled in the gate area. This change may be attributed to the varying surface potential of the electrolyte solution for different pH levels [20]. Figure 2 shows the threshold voltage of the device with varying pH level of the electrolyte solution [20].

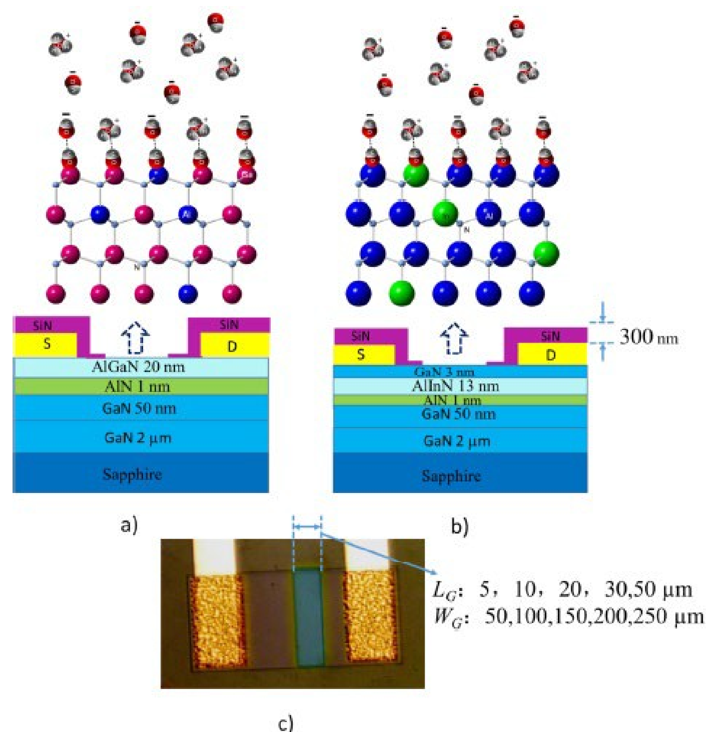

Figure 1. (**a**) Schematic illustration of the AlGaN/GaN heterostructure open gate pH sensor and the graphic representation of reactions between the POH groups on the sensing surface and other ions in the aqueous solution, where Ga, Al and N atoms are represented by pink, blue and light blue. (**b**) Schematic illustration of the AlInN/GaN heterostructure open gate pH sensor and the graphic representation of the reactions between the POH groups on the sensing surface and other ions in the aqueous solution, where Al, In and N atoms are represented by blue, green and light blue. The hydrone (water molecules), hydrion (H ion) and hydroxyl ion are shown; O and H are represented by red and gray. (**c**) top view of one fabricated device [20,64]

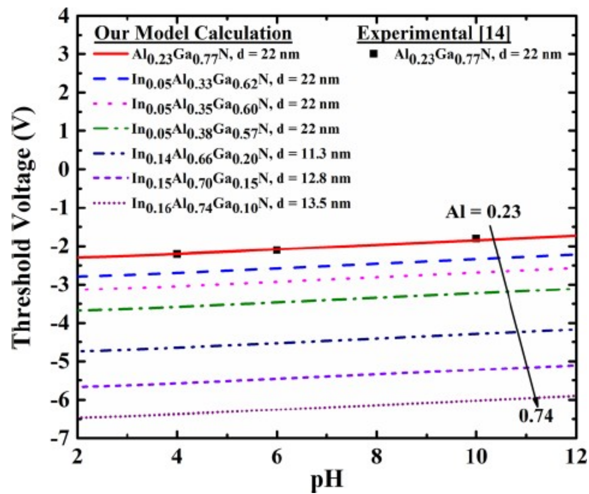

Figure 2. Threshold voltage of the device with varying pH level of the electrolyte solution [20]

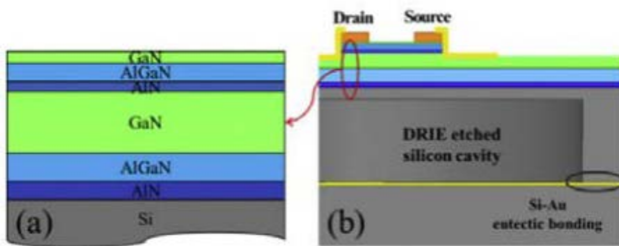

Figure 3. (a) Schematic of the AlGaN/GaN heterostructure sensor (b) Section diagram of the AlGaN/GaN pressure sensor [3]

The result of that work proposed an In and Al composition dependent unified analytical model for pH sensing applications of InAlGaN/GaN HEMTs [20]. Figure 3 shows the AlGaN/GaN Hetrostructure sensor (a), and (b) shows the section diagram of the AlGaN/GaN pressure sensor (3). The impact of the change in mole fraction of Al, In and electrolyte pH level on the threshold voltage and the drain current of various device structures has been examined [20]. They verified that by utilizing suitable In and Al compositions, high concentration of the 2DEG can be obtained in the InAlGaN/GaN heterostructures even with a thin barrier layer. The InAlGaN/GaN devices have slightly higher negative threshold voltage than the conventional AlGaN/GaN HEMTs due to its high 2DEG concentration. The sensitivity of an HEMT based pH sensor is dependent on its transconductance. The maximum transconductance of the AlGaN/GaN devices was found to be much lower than that of the InAlGaN/GaN HEMTs [20]. The thinner barrier layer of the InAlGaN/GaN HEMTs enhance the gate control capability and the transconductance of the device. Increased maximum transconductance in quaternary InAlGaN/GaN leads to enhanced sensitivity to the pH levels of the electrolyte. Therefore, they concluded that exploiting the InAlGaN devices for pH measurement applications can result in better performance [20]. The analytical results showed good agreement with the experimental results available in the literature. The average measurement was found to be miniscule 0.0070 [20]. They expected their model to be a useful tool to predict the behaviour of HEMTs in different acidic environments and to have applications in device optimization and sensor calibration purposes for future chemical and biochemical sensors [20]. The only shortcoming of that model is to recognize the acceptable approximate values of fitting parameters used [20].

In recent years, considerable attention has been turned to the nanostructures as chemical sensors due to their simple and low-cost operation, fast response, easy production, and high surface-to-volume ratio [25]. The work of Density Functional Theory (DFT) calculation in chemical sensing was investigated and reported by Elesawya et al. [25]. In that work, they employed the DFT calculations to investigate the interaction between SA (antibiotic, sulfonamide) and Au-decorated gallium nitride nanotube (GaNNT) as pristine nanotube [25]. Different methods have been previously employed for the detection of sulfonamide (SA), namely static SIMS, gas chromatography, HPLC, and ion-exchange chromatography [26,27,28]. That work resulted in enhanced sensitivity in comparison with simple Schottky diodes which are fabricated on other layers of group III-nitrides [25]. The pristine GaNNT could not sense SA, but after the Au atom was decorated, the sensitivity of the GaNNT to SA increased significantly. Also, after the Au atom was decorated, E_{ad} of SA decreased from -6.0 to -22.9 kcal/mol. The sensing response (SR) of the Au at GaNNT was 98.1, which was considerable. The E_{ad} of SA was reduced by the water solvent to -19.1 kcal/mol [25]. In addition, SA was desorbed from the surface of the decorated nanotube with the recovery time of 4.9 s at ambient temperature [25]. Therefore, we can conclude that the Au at GaNNT can be utilized in manufacturing promising sensors to detect SA [25]. Figure 4 illustrates the partial DOS of the most stable Sulfonamide/Au-decorated GaNNT complex. In that figure we can see the energy vs. DOS variations of both HOMO and LUMO curves.

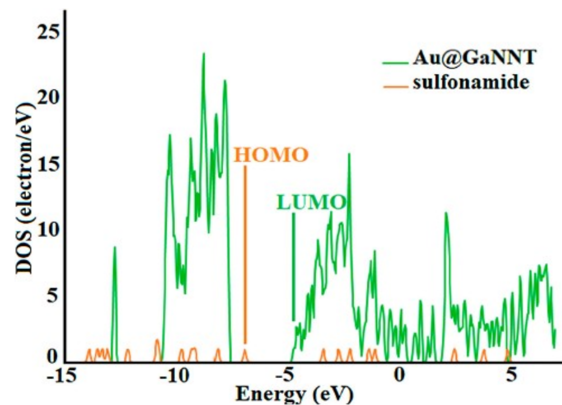

Figure 4. Partial DOS of the most stable sulfonamide/Au-decorated GaNNT complex [25]

The application of GaN in using selective annealing to produce Schottky-Type Sensor was reported by Park et al. [29]. Figure 5 presents the fabrication process of the Pt/GaOx/GaN-based Schottky diode sensor [3,20,32]. That work showed how using selective annealing improved the performance of the sensor and improved its dark current density from 1.3 X 10^{-7} A/cm^2 to 8.5 X 10^{-10} A/cm^2 [29]. The results of a transmission electron microscopy analysis demonstrated that the annealing process caused interdiffusion between the metal layers; the contact behavior between Ti/Al/Ni/Au and AlGaN changed from rectifying to ohmic behavior [29]. Nitride-based semiconductors have been broadly used in important applications such as high-power/high-speed electron devices, visible/UV laser diodes, LEDs, and UV sensors [30,31,32].

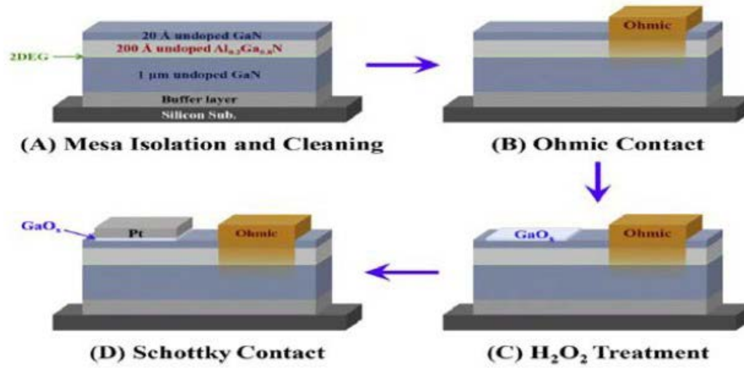

Figure 5. Fabrication of the Pt/GaOx/GaN-based Schottky diode sensor [3,20,32]

Recent studies have intensely explored device structures and experimental techniques to improve the performance of UV sensors [29,33,34]. Selective thermal annealing exploits Joule heating via a current that is generated following the local breakdown of the insulator in a metal-insulator-metal structure. In that work, they investigated the effects of selective annealing on asymmetric MSM ALGaN/GaN UV sensors that were epitaxially grown on a sapphire substrate and have all compositions of 24% [29]. Figure 6 shows a schematic of the asymmetric MSM AlGaN UV sensor with 24% A [29]. The dummy pad is showed on the top of the device [29]. The dummy pad also shown from a magnified image in Figure 7.

They used a Ti/Al/Ni/Au metal scheme in the sensors that minimized the degradation of device performance and exhibited reasonable ohmic behavior after selective annealing [29]. The electrical and UV optical characteristics were analyzed both before and after selective annealing to enable a comparison [29].

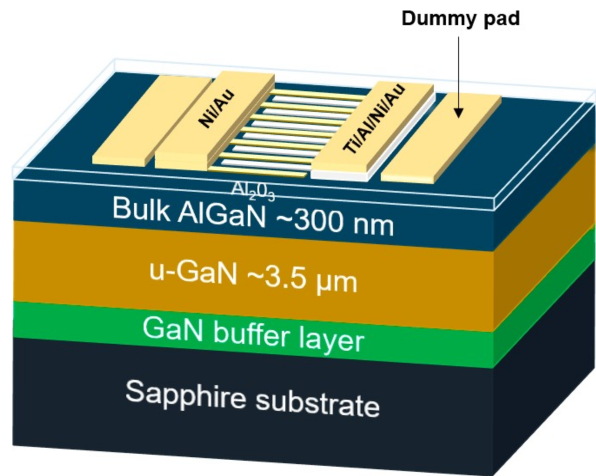

Figure 6. Schematics of the asymmetric MSM AlGaN UV sensor with 24% A [29]

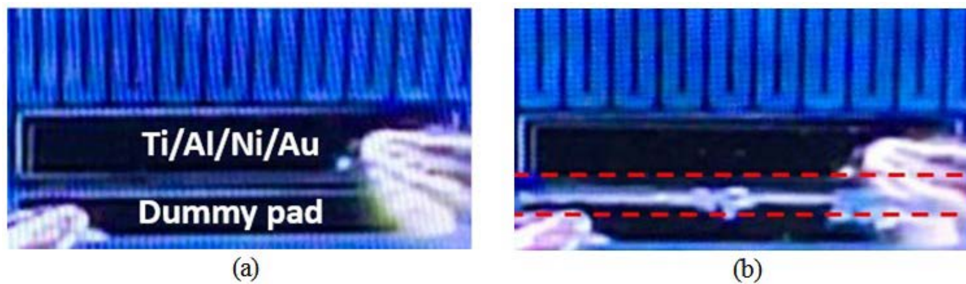

Figure 7. Images magnified 90x using a photomicroscope of MS TECH's MST-8000C probe station: top views of an asymmetric MSM AlGaN UV sensor (a) before and (b) after selective annealing (annealed region is marked with dotted box) [29]

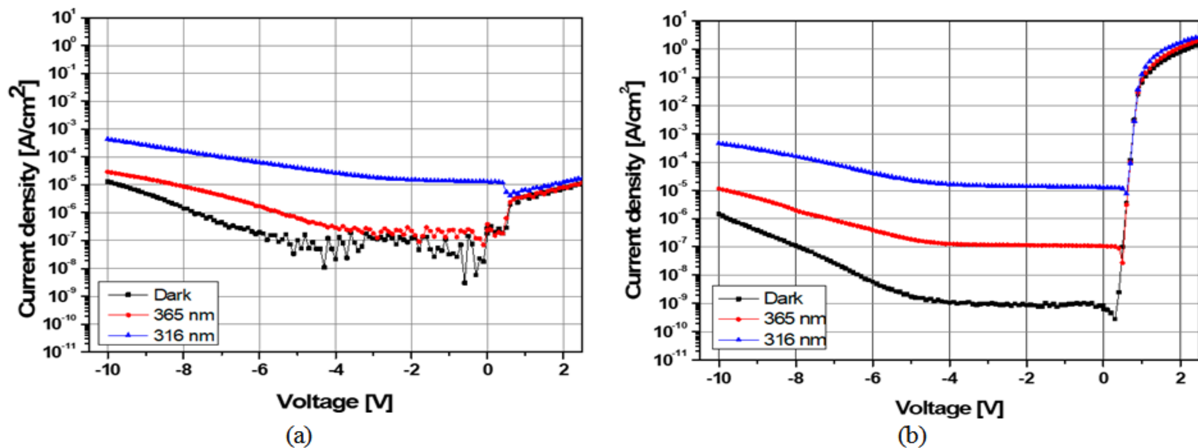

Figure 8. Dark state and UV photo responsive I-V of the asymmetric MSM AlGaN UV sensor (a) before and (b) after selective annealing [29]

As shown in Figure 8 (a,b) under forward bias, the selective annealing process changes the rectifying contact of Ti/Al/Ni/Au electrode to near ohmic contact, which is suspected originated from the formation of nitrogen vacancies [29]. During annealing, N easily reacts with Ti to form TiN, and the remaining nitrogen vacancies serve as donors on the AlGaN substrate and promote high electron concentration. That work showed the changes the contact behaviour by reducing the Schottky barrier in the Ti/Al/Ni/Au electrode [29]. Thus, the application of a reverse bias at the Ni/Au electrode would cause electrons captured by the interfacial traps to be emitted by trap-assisted tunnelling, thereby contributing to the leakage current. Selective annealing is thought to passivate and reduce interfacial traps, thus resulting in a lower dark current density [29].

The conclusion of that work was that under a forward bias of 2.0 V, the selective annealing substantially increased the dark current density from 7.6 X 10^{-6} A/cm^2 to 0.8 A/cm^2, which was attributed to nitrogen vacancies generated by the selective annealing that altered the contact behaviour of the Ti/Al/Ni/Au electrode. Under reverse bias, the dark current density at a bias of -2.0 V. was 8.5 X 10^{-10} A/cm^2 and the UVRR at a bias of -7.0 V was 672 [29]. The results of the XPS analysis of the sensors showed that annealing reduced the peak intensity of the O 1s binding energy associated with Ga oxide on the AlGaN surface from around 846 to 598 counts/s [29]. These results demonstrated a remarkable performance improvement because of the selective annealing, which probably arose from surface passivation and a reduction in the number of traps at the metal/AlGaN interface [29]. These results suggested that selective annealing by dielectric breakdown is a facile technique involving localized heating that does not require additional fabrication processing steps or equipment and shows it is useful for improving the performance of sensor devices [29]. Recently, a selective annealing method that employs dielectric breakdown changed the contact behavior of a nitride-based UV sensor, but the structural and electrical effects of the selective annealing process are not well understood [35]. Figure 9 shows an image of the annealed ZnO on sapphire substrate [3,35].

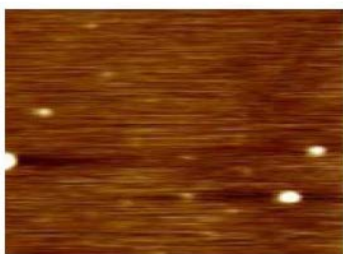

Figure 9. AFM images of the annealed ZnO on sapphire substrate [3,35]

Piezoelectric multilayers are widely used in high-performance sensors, actuators, and optoelectronic devices [36]. Piezoelectric multilayer actuators are being used in various applications because of their low drive voltage, high energy density, quick response, and long lifetime [36]. The application of GaN in analytical solutions of electro elastic fields in piezoelectric thin-film multilayer was reported and investigated by Mishra et al. [36]. In that work they studied the applications to piezoelectric sensors and actuators [36]. The inherent piezoelectric properties of these devices lead to the coupled electro elastic fields generated in each layer [36]. In electronic applications such as GaN-based high electron mobility transistors (HEMT) and LEDs, the multiquantum wells (MQWs) can have different lattice parameters and thermal expansion coefficients that give rise to lattice misfit and thermal strains [36]. Since the strains and electric fields in the layers can influence the electromechanical or optoelectronic device performance, the accurate quantification of their magnitudes is of great importance [36]. They can also be important in quantifying the formation of defects and predicting their densities [36]. Therefore, it will be useful to derive analytical expressions based on the constitutive relations that can readily quantify the electro elastic fields in the piezoelectric multilayer [36]. Figure 10 (a,b) represents a schematic representation of a multilayer piezoelectric actuator with opposite poling, out-of-plane normal strain (εzz) for Z-stack multilayer actuator [36].

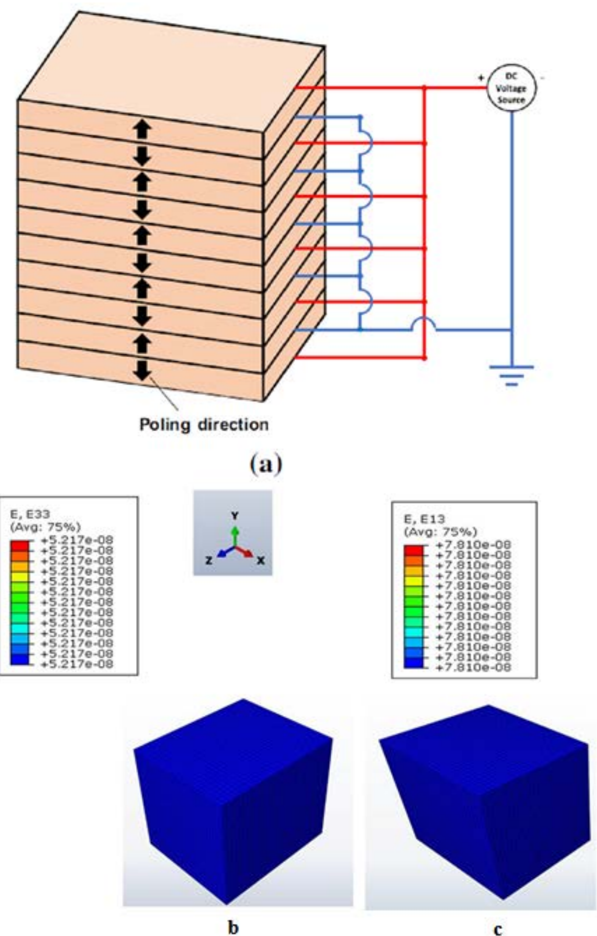

Figure 10. a. Schematic representation of a multilayer piezoelectric actuator with opposite poling, **b.** out-of-plane normal strain (εzz) for Z-stack multilayer actuator, **c.** out-of-plane shear strain (εxz) for Y-stack multilayer actuator [36]

The analytical prediction methodology developed herein can be useful in electromechanical and optoelectronic device design, especially when piezoelectrically generated electro elastic fields have to be taken into account [36]. In that work, they derived the analytical expressions for electro elastic fields in piezoelectric multilayers subjected to external force, moment, and electric potential along with the lattice and thermal mismatches between the reference substrate and the deposited film layers [36]. Results for the purely elastic isotropic multilayer can be

deduced by letting the elastic constants be isotropic and letting the piezoelectric terms vanish [36]. Different types of piezoelectric sensors and actuators were also modelled using the commercial finite element analysis code ABAQUS 6.14 to validate the analytical results. Excellent agreements between the analytical and FEM results were observed for all applications considered in their work [36]. Their work can be useful in designing electromechanical devices by providing quick and accurate electro elastic field results for piezoelectric multilayers [36].

The resistance strain gauge was invented by Simmons and Ruge in 1938 [38], and it has been nearly 80 years since resistance strain force sensors began to be produced in 1942. Force sensors based on resistance strain gauges have been widely used in the stress tests of various components and structures in the aerospace, transportation and automobile industries, civil engineering, and even the medical field [37]. For example, in civil bridge structures, the great amount of strain acting on the bridge structure over a long time will fatigue the structure and yield a fracture [37]. A strain sensor based on a resistance strain gauge can measure not only the strain on the surface of the structure but also the strain inside the structure [37]. When the strain gauge is embedded in poured concrete structures, the strain state inside these structures can be monitored in real time through external measuring lines [39]. The study of Development and Application of Resistance Strain Force Sensors was presented by Zhao et al. [39]. In that work, they reviewed the recent progress of the micro-nano structure of resistance strain-sensitive grids and the strain transfer characteristics of the strain-type force sensor. Further, the technical developments and key problems of resistance strain force sensors for their future application demands were explored [37].

Silver nanoparticles and carbon nanotubes are in development for compressible flexible piezoresistive sensors [40]. To overcome the hinders on the progress of nanodevice fabrication, significant efforts have been expended on the production of CNTs macrostructures [41]. Inkjet printing techniques have provided outstanding results for flexible resistance sensors in terms of their resistance reproducibility [42].

Interesting, the coupling effects among the physical effects, such as coupling piezo resistivity with piezoelectricity, have emerged to be a promising approach to boot the sensitivity effect [37]. A giant piezoresistive effect resulting from the optoelectronic coupling in a cubic silicon carbide/silicon heterojunction gives rise to a gauge factor of 58,000, which is more than 2000 times greater than that of cubic silicon carbide [43]. By sufficiently finely tuned nanowires in uniform phase-change materials thin films, its significant piezoresistive effect gives rise to a giant gauge factor of 338 used in integrated flexible tactile sensors [44]. The strain transfer and creep characteristics of strain sensors are the key factors that determine the sensitivity coefficient, mechanical lag, and long-term stability of strain sensors [37]. Future work should be carried out in such fields as the ingredient technologies for sensitive grid materials, forging manufacturing technology, heat treatment and mechanical stability technology, and surface treatment technology for improving the characteristics of sensitive grid materials [37].

The study of Electrodeposition of Pd-Pt Nanocomposites on Porous GaN for Electrochemical Nitrite Sensing was reported and investigated by Rui et al. [45]. In that work, they exhibited a novel Pd-Pt nanocomposite-modified PGaN electrode through a simple two-step electrochemical deposition route for nitrite sensing [45]. Due to their excellent electrocatalytic activities, noble metal nanomaterials have been applied to composite electrochemical sensors [46,47]. For the high-porosity structure that uses PGaN as a supporting electrode and for the effective electronic transmission of Pd-Pt nanocomposites, the Pd-Pt/PGaN nitrite sensor presented many features, such as a wide linear range, high sensitivity, good selectivity and stability [45]. Figure 11 presents an SEM image (a) and aperture distribution histogram (b) of PGaN electrode [44]. Furthermore, it can detect the nitrite in tap and lake water, respectively. The simply assembled Pd- Pt/PGaN sensor provides a fast and effective method for monitoring nitrite in a realistic environment [45].

The application of GaN as a pH Sensor was reviewed and reported by Khalifa et al. [48]. In their work, they presented the GaN/Al_2O_3-based EGFET pH sensor. Figure 13 showed the IDS-VREF characteristics in the linear region at VDS = 0.3 V [50]. The study concluded a positive and negative linear correlation with superior linearity 0.98 between the reference voltage (VREF) and the drain-source current (IDS), respectively, versus pH value [48]. The sensing system used a high-performance cavity according to Ahmed et al. [49]. The voltage sensitivity was 24.72 mV/pH, while the current sensitivity obtained 0.39 (μA)1/2/pH [48]. The main important factor as an indicator for stability and reversibility to field effect transistors in applications of ion detecting is the hysteresis phenomenon [48]. The hysteresis depths at pH 7 in cycle 7-4-7-10-7 were 14.98 mV and 30.91 mV for acidic and basic sides, respectively [48]. The results showed stable detecting executions which qualify the GaN/Al_2O_3-based EGFET pH sensor to be used for commercial devices. Figure 13 shows the I_{DS}-V_{REF} characteristics in the linear region at V_{DS} = 0.3 V [50].

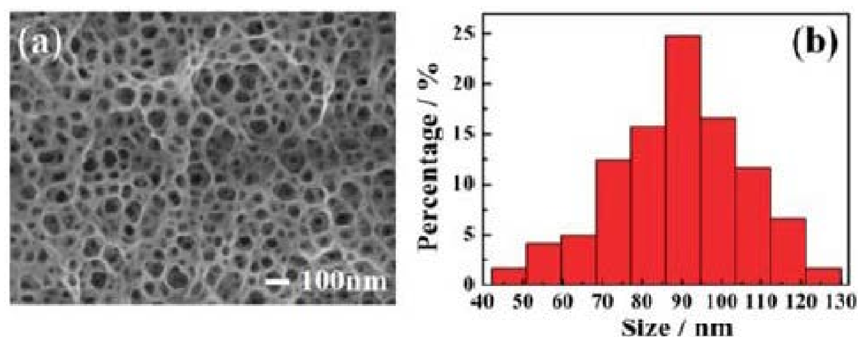

Figure 11. a. SEM image and **b**. aperture distribution histogram of PGaN electrode [44]

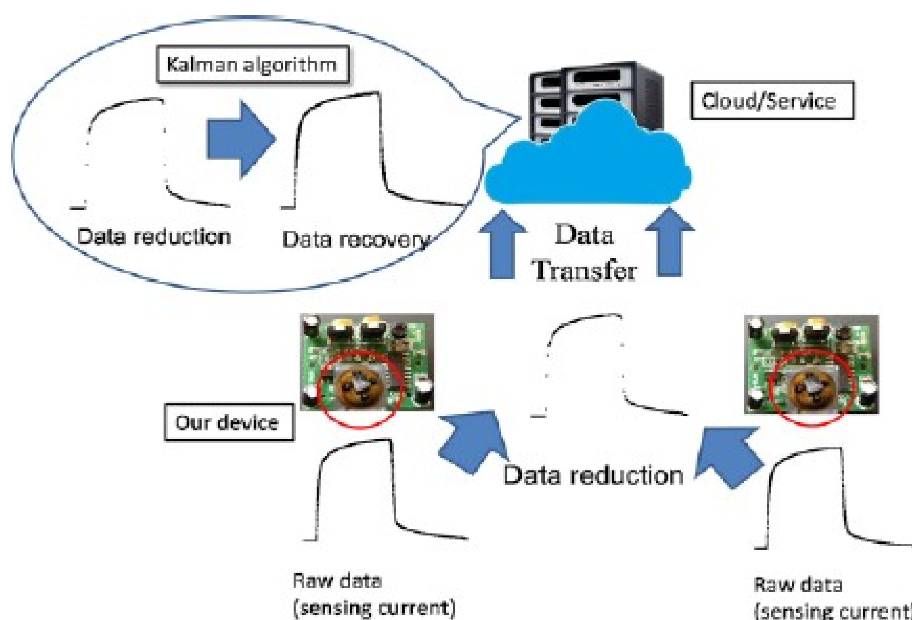

Figure 12. Schematic diagram of sensing transmission structure of the GaN sensor for IoT applications [3,48]

The equation that describes behavior I_{DS} versus V_{Ref} in the linear region can be expressed as in equation 1.

$$I_{DS} = K_M \left[2\left(V_{\mathrm{Ref}} - V_{\mathrm{Th}}\right) V_{\mathrm{DS}} - V_{\mathrm{DS}}^2 \right]^4 \quad (1)$$

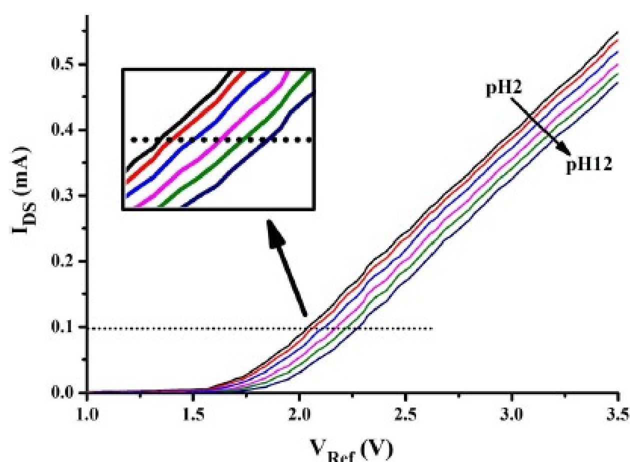

Figure 13. I_{DS} vs. V_{Ref} characteristics of (EGFET) GaN/Al_2O_3 [50]

In addition, size controlling of sensing area, long sensing of pH range, good repetition accuracy, and the features of GaN such as not toxic material give this sensor a good level of practicability [45].

A review for GaN gas sensing properties was reported and studied by Ashfaque et al. [51]. In their work, they reviewed and categorized the progress in GaN nanostructures-based sensors for detection of gas/chemical species such as hydrogen (H_2), alcohols (R-OH), methane (CH_4), benzene and its derivatives, nitric oxide (NO), nitrogen dioxide (NO_2), sulfur-dioxide (SO_2), ammonia (NH_3), hydrogen sulfide (H_2S) and carbon dioxide (CO_2) [51]. That work showed that the Internet of Things (IoT) applications required ultra-low power, mini-sized chemical sensors, which are easily integrated into electronic circuits for remote air quality monitoring in automated systems [51,52]. Figure 12 shows a representation of the sensor in the IoT network in general view. Although GaN nanostructures have been very suitable for hydrogen and alcohol sensing, detection of various oxidizing gases was also demonstrated [51]. Also, the device performance was degraded very little when exposed to siloxane for a one-month period [51].

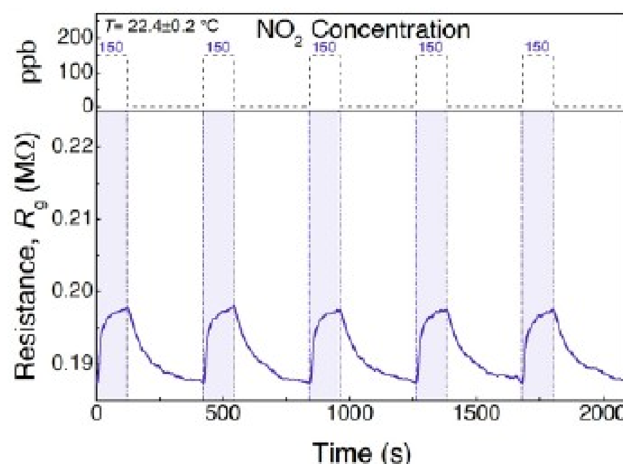

Figure 14. Repeatability of VHD gas sensor exposed to 150 ppb of NO_2 of GaN sensor [3,51]

Nanostructures are suitable candidates for this type of sensing application. The standard sensing performance parameters like limit of detection, response/recovery time and operating temperature for different types of sensors and structures were summarized comprehensively for the comparative study [51]. The proposed metric, product of response time and limit of detection, has been calculated for each sensor to measure and compare the overall sensing performance among reported GaN nanostructures-based devices so far [51]. Based on the analysis of sensing characteristics and the proposed metric, it was found that InGaN/GaN NW sensor showed superior overall sensing performance for H_2 gas sensing [51]. Also, GaN/TiO_2-Pt) and GaN/TiO_2 NWNC sensors were highly suitable for ethanol and TNT sensing, respectively [51]. Moreover, metal-oxide coated GaN NWs exhibit reliable sensing performance toward various oxidizing gases including NO_2

and SO_2 [51]. Theoretical studies on molecular models of gas molecules and GaN have been reviewed [51]. Artificial neural networks (ANNs) have been highly efficient to capture the non-linear response pattern of gas mixtures [51]. Furthermore, a brief analysis of the implementation of machine learning on GaN nanostructured sensors and sensor array has been presented [51]. In addition, gas sensing mechanisms of the GaN sensors have been discussed. This overview on the GaN nanostructures-based gas sensors is helpful for the researchers to gain a quick understanding of the status of GaN nanostructure- based sensors [51]. Figure 14 shows a schematic of repeatability of VHD gas sensor exposed to 150 ppb of NO_2 of GaN sensor [3,51].

Having a large surface-to-volume ratio, nanostructures such as nanowires, nanorods, nanotubes, nanoparticles and nanobelts favor adsorption of gas molecules on the sensor and thus increase the sensitivity of the device [51,53]. Although commercially available metal-oxide nanostructure- based gas sensors show high sensitivity and low detection limits [51,52,53,54], poor analyte selectivity, high operating temperature, and unstable performance in harsh environments [54]. Recently, porous GaN nanorods were prepared by a hydrothermal method by Zhang et al. [55]. Gas-sensing measurements indicated that the porous sensor exhibits high sensitivity and strong selectivity to ethanol, and good stability at high temperature (360 C). They presented a new route for the synthesis of GaN submicron rods [56]. P-i-n GaN nanorods (NRs), comprising of InGaN/GaN multi-quantum wells, have been reported recently for NO gas sensing [57]. In another study, GaN nanowires were attached on pencil graphite electrodes using a hydrothermal method for NO detection [58]. The ppb level of NO_2 was demonstrated by titania (TiO_2) nanoclusters-functionlized GaN submicron wire fabricated by a top-down approach [59]. Previously, Shi et al. [60] fabricated hybrid gas sensors based on TiO_2-decorated GaN nanowires for NO_2 detection. In another work, GaN nanowires were developed on Si substrates using stepper lithography assisted dry-etching in a top-down fabrication approach [61]. The work reported by Thomson et al. showed fabricated GaN submicron wire-based chip-scale, low-power and nanoengineered chemiresistive gas-sensing architecture for CO_2 detection [62]. Recently, a gas sensor array was reported comprising of GaN nanowires functionalized with metal incorporated TiO_2 and ZnO [63]. In another study, various artificial neural network (ANN) algorithms were trained and tested for the identification and quantification of gas mixtures based on GaN nanowires [64].

4. Conclusion

This paper presented and reviewed the recent advances of GaN fabrication and applications. Fabrication and growth of GaN devices was discussed in addition to the recent technologies of doping processes. The applications of GaN was presented and emphasized in this work. GaN sensors and detectors were discussed in detail with recent discoveries and investigations. Despite this progress, still some aspects of GaN devices and structures to be developed to meet further commercial and technological interests. The planar GaN based gas sensors have high restrictions to the detection of low gas concentrations. Moreover, GaN based sensors sensitivity, speed (response and recovery rates), selectivity, stability, reproducibility, durability, detection limit, and power consumption need more investigation and development. There is still much to be discovered in terms of the mechanism of GaN based sensor devices, specially for hydrogen gas sensors. Hence, the development of the high- performance hydrogen gas sensors to continuously monitor the leakage of hydrogen and to accurately detect hydrogen concentration is an important and crucial issue in terms of environmental safety. Finally, although several GaN based sensors devices have been used and commercialized, still some drawbacks and issues to be resolved with intense investigation and research. These issues include the *p*-type doping, the lack of a credible *p*-type doping hampers widespread optical emitters in GaN.

References

[1] Liu, X., Yang, X., Yang, X., Lv, B., Luo, Z. "Exploration of N- and p-type doping for two-dimensional gallium nitride: Charged defect calculation with first principles." The European Physical Journal B 93, 8-10 (2020).

[2] Zhang, X., Jin, L., Dai, X., Chen, G., Liu, G. "Two-Dimensional GaN: An Excellent Electrode Material Providing Fast Ion Diffusion and High Storage Capacity for Li-Ion and Na-Ion Batteries" Appl. Mater. Interfaces 10.38978, (2018).

[3] Nahhas, A. M. "A Review of GaN Nanowires Based Sensors." American Journal of Nanomaterials 1. 32-47, (2020).

[4] Sun, R., Wang, G., Peng, Z. "Fabrication and UV photo response of GaN nanowire-film hybrid films on sapphire substrates by chemical vapor deposition method." Materials Letters 217-288-291, (2018).

[5] Quang, B., Ludovic, L., Martina, M., Nikoletta, J., Olivia, M., Laurent, T., Xavier, L., Christophe, D., Jean, H., Maria, T., Noelle, G. "GaN/Ga_2O_3 Core/Shell Nanowires Growth: Towards High Response Gas Sensors." Applied Sciences. 9-3528, (2019).

[6] Thakur, D., Sharma, A., Awasthi, A., Rana, D., Singh, D., Pandey, S., Thakur, S. "Manganese-Doped Zinc Oxide Nanostructures as Potential Scaffold for Photocatalytic and Fluorescence Sensing Applications." Chemosensors 8-120, (2020).

[7] Pandey, S., Fosso, E., Spiro, M., Waanders, F., Kumar, N., Ray, S., Kim, J. "Equilibrium, kinetic, and thermodynamic studies of lead ion adsorption from mine wastewater onto MoS_2-clinoptilolite composite", Materials Today Chemistry 18-100376, (2020).

[8] Maity, S., Ramanan, C., Ariese, F., MacKenzie, R. C. I., von, E. "In Situ Visualization and Quantification of Electrical Self-Heating in Conjugated Polymer Diodes Using Raman Spectroscopy." Advanced Electronic Materials 8-2101208, (2022).

[9] Arivazhagan, L., Nirmal, D., Reddy, K., Ajayan, J., Godfrey, D., Prajoon, P., Ray, A. "A Numerical Investigation of Heat Suppression in HEMT for Power Electronics Application" Silicon 13-3039, (2020).

[10] Huang, D., Sun, Q., Liu, Z., Xu, S., Yang, R., Yue, Y. "Ballistic Thermal Transport at sub-10 nm laser-induced hot spots in GaN Crystal" Advanced Science 10, 202204777, (2022).

[11] Sena, H., Atsushi, T., Yotaro, W., Tomomi, A., Toshiki, Y., Daisuke, K., Ryuji, S., Yoshio, H., Yasunori, I., Hiroshi, A. "Gallium nitride wafer slicing by a sub-nanosecond laser: effect of pulse energy and laser shot spacing" Applied Physics A, 127-648, (2021).

[12] Sodre, J., Longo, E., Taft, C., Martins, J., Santos, J. "Electronic structure of GaN nanotubes." Comptes Rendus Chimie 20-190-196, (2017).

[13] Lee, M., Mikulik, D., Park, S. "Thick GaN growth via GaN nanodot formation by HVPE." CrystEngComm 19-930-935, (2017).

[14] Reddeppa, M., Park, B., Lee, S., Hai, N., Kim, M. "Improved Schottky behavior of GaN nanorods using H_2 plasma treatment." Current Applied Physics 17-192-196, (2017).

[15] Narita, T., Kataoka, K., Kanechika, M., Kachi, T., Uesugi, T. “Ion implantation technique for conductivity control of GaN.” 17th International Workshop on Junction Technology (IWJT) 87-90, (2017).

[16] Narita, T., Kachi1, T., Kataoka, K., Uesugi, T. “P-type doping of GaN(0001) by magnesium ion implantation.” Applied Physics Express 10-16501, (2017).

[17] Liu, X., Yang, X., Yang, X., Bing, L., Zijiang, L. “Exploration of n- and p-type doping for two-dimensional gallium nitride.” The European Physical Journal B 93-148, (2020).

[18] Wang, X., Xu, L., Jiang, Y., Yin, Z., Chan, C., Deng, R. “III-V compounds as single photon emitters.” Journal of Semiconductors 40-071906, (2019).

[19] Manjakkal, L., Szwagierczak, D., Dahiya, R. “Metal oxides based electrochemical pH sensors: Current progress and future perspectives.” Progress in Materials Science 109-100635, (2020).

[20] Upadhyay, K., Chattopadhyay, Manju, K. “A Composition-Dependent Unified Analytical Model for Quaternary InAlGaN/GaN HEMTs for pH Sensing.” Journal of Electronic Materials 50, 3392-3405, (2021).

[21] Khan, M. I., Mukherjee, K., Shoukat, R., Dong, H. “A review on pH sensitive materials for sensors and detection methods.” Microsystem Technologies 23-4391, (2017).

[22] Ghoneim, M. T., Nguyen, A., Dereje, N., Huang, J., Moore, G. C., Murzynowski, P. J., Dagdeviren, C. “Recent Progress in Electrochemical pH-Sensing Materials and Configurations for Biomedical Applications.” Chemical Reviews 119-5248, (2019).

[23] Sanyal, I., Lee, Y. C., Chen, Y. C., Chyi, J. I. “Achieving high electron mobility in AlInGaN/GaN heterostructures: The correlation between thermodynamic stability and electron transport properties.” Applied Physics Letters 114-222103, (2019).

[24] Shrestha, N. M., Chen, C. H., Tsai, Z. M., Li, Y., Tarng, J. H., Samukawa, S. “Barrier Engineering of Lattice Matched AlInGaN/ GaN Heterostructure Toward High Performance E-mode Operation.” International Conference on Simulation of Semiconductor Processes and Devices (SISPAD) 1-4, (2019).

[25] Basem, H., Ahmad, A., Nasser, S., Hala, A., Ibrahium, P. D., Nezhad, Mohd, S. “A density functional theory study of Au-decorated gallium nitride nano-tubes as chemical sensors for the recognition of sulfonamide.” Journal of Sulfur Chemistry, (2022).

[26] Zhao, T., Wang, M., Chu, Y. “On the Bounds of the Perimeter of an Ellipse.” Acta Mathematica Scientia 42:491-501, (2022).

[27] Zhao, T., Wang, M., Hai, G. “Landen inequalities for Gaussian hypergeometric function”, Serie A. Mathematics 116, 1-23, (2021).

[28] Nazeer, M., Hussain, F., Khan, M. “Theoretical study of MHD electro-osmotically flow of third-grade fluid in micro channel.” Applied Mathematics and Computation 420:126868, (2022).

[29] Park, B., Seol, J., Hahm, H. “A Schottky-Type Metal-Semiconductor-Metal Al0.24Ga0.76N UV Sensor Prepared by Using Selective Annealing.” Sensors 21-4243, (2021).

[30] Lee, C. J., Won, C. H., Lee, J. H., Hahm, S. H., Park, H. “GaN-Based Ultraviolet Passive Pixel Sensor on Silicon (111) Substrate.” Sensors 19-1051, (2019).

[31] Lee, C. J., Won, C. H., Lee, J. H., Hahm, S. H., Park, H. “Selectively Enhanced UV-A Photoresponsivity of a GaN MSM UV Photodetector with a Step-Graded AlxGa1-xN Buffer Layer.” Sensors 17-1684, (2017).

[32] Chiu, Y. C., Yeh, P. S., Wang, T. H., Chou, T. C., Wu, C. Y., Zhang, J. J. “An Ultraviolet Sensor and Indicator Module Based on p-i-n Photodiodes.” Sensors 19-4938, (2019).

[33] Chang, S., Chang, M., Yang, Y. “Enhanced Responsivity of GaN Metal-Semiconductor-Metal (MSM) Photodetectors on GaN Substrate.” IEEE Photonics Journal, 9-7, (2017).

[34] Nallabala, N. K. R., Godavarthi, S., Kummara, V. K., Kesarla, M. K., Saha, D., Akkera, H. S., Guntupalli, G. K., Kumar, S., Vattikuti, S. V. P. “Structural, optical and photoresponse characteristics of metal-insulator-semiconductor (MIS) type Au/Ni/CeO_2/GaN Schottky barrier ultraviolet photodetector.” Materials Science in Semiconductor Processing 117-105190, (2020).

[35] Seol, J. H., Hahm, S. H. “Selective Ohmic Contact Formation on Schottky Type AlGaN/GaN UV Sensors Using Local Breakdown.” Materials Science in Semiconductor Processing 19-2946-2949, (2019).

[36] Dhaneshwar, M., Sung, Y., Youjoung, S., Eugene, P. “Analytical solutions of electroelastic fields in piezoelectric thin- film multilayer: applications to piezoelectric sensors and actuators.” Acta Mechanica 231-1435-1459, (2020).

[37] Yinming, Z., Yang, L., Yongqian, L., Qun, H. “Development and Application of Resistance Strain Force Sensors.” Sensors 20-5826, (2020).

[38] Zhang, C., Ge, Y., Hu, Z., Zhou, K., Ren, G., Wang, X. “Research on deflection monitoring for long span cantilever bridge based on optical fiber sensing.” Optical Fiber Technology 11-200-202, (2019).

[39] Zheng, F., Wu, Y., Zhang, J., Yang, X. “Piezoresistive flexible sensor based on single wall carbon nanotubes.” Sensors, 32-1009-1015, (2019).

[40] Bishop, M. D., Hills, G., Srimani, T. “Fabrication of carbon nanotube field-effect transistors in commercial silicon manufacturing facilities.” Nature Electronics 3-492-501, (2020).

[41] Bodelot, L., Pavic, L., Hallais, S., Charliac, J., Lebental, B. “Aggregate-driven reconfigurations of carbon nanotubes in thin networks under strain: In-situ characterization.” Scientific Reports 9-1-11, (2019).

[42] Nguyen, T., Dinh, T., Foisal, A., Phan, H., Nguyen, T., Nguyen, N., Dao, D. “Giant piezoresistive by optoelectronic coupling in a heterojunction.” Nature Communications 10-4139, (2019).

[43] Wang, Z., Dong, C., Wang, X., Li, M., Nan, T., Liang, X., Chen, H., Wei, Y., Zhou, H., Zaeimbashi, M. “Highly sensitive integrated flexible tactile sensors with piezoresistive CST thin films.” Flexible Electronics 2-17, (2018).

[44] Rui, X., Shao, Z., Long, Z., Chao, W., Lu, W., Jing, Y. “Electrodeposition of Pd-Pt Nanocomposites on Porous GaN for Electrochemical Nitrite Sensing.” Sensors 19-606.0.3390/s19030606, (2019).

[45] Shahrokhian, S., Rezaee, S. “Vertically standing Cu_2O nanosheets promoted flower-like PtPd nanostructures supported on reduced graphene oxide for methanol electro-oxidation. Electrochim.” Electrochimica Acta 259-36-47, (2018).

[46] Zheng, J., Wang, B., Ding, A., Bo, W., Chen, J. “Synthesis of MXene/DNA/Pd/Pt nanocomposite for sensitive detection of dopamine” Journal of Electroanalytical Chemistry 816-189-194, (2018).

[47] Ali, M., Ali, H., Hajer, Z., Naser, M. “Extended Gate Field Effect Transistor-Based n-Type Gallium Nitride as a pH Sensor.” Journal of Electronic Materials 50 7071-7077, (2021).

[48] Ahmed, N. M., Sabah, F. A., Al-Hardan, M. A. Almessiere, S. M. Mohammad, W. F., Lim, M., Jumaah, A. S., Islam, Z., Hassan, H. J., Afzal, N. “Development of EGFET-based ITO pH sensors using epoxy free membrane.” Semiconductor Science and Technology 36-045027, (2021).

[49] Palit, S., Singh, K., Lou, B. S., Her, J. L., Pang, S. T., Pan, T. M. “Ultrasensitive dopamine detection of indium-zinc oxide on PET flexible based extended-gate field-effect transistor.” Sensors and Actuators B: Chemical 310-127850, (2020).

[50] Khan, M., Mulpuri, V. “Gallium Nitride (GaN) Nanostructures and Their Gas Sensing Properties: A Review”, Sensors 20-3889, (2020).

[51] Gomes, J. B. A., Rodrigues, J. J. P. C., Rabelo, R. A. L., Kumar, N., Kozlov, S. “IoT-Enabled Gas Sensors: Technologies, Applications, and Opportunities.” Journal of Sensor and Actuator Networks 8-57, (2019).

[52] Rani, A., DiCamillo, K., Khan, M. A. H., Paranjape, M., Zaghloul, M. E. “Tuning the Polarity of $MoTe_2$ FETs by Varying the Channel Thickness for Gas-Sensing Applications.” Sensors 19-2551, (2019).

[53] Sarf, F. “Metal Oxide Gas Sensors by Nanostructures” Gas Sensors, Ch.2, P.3, (2020).

[54] Zhang, M., Zhao, C., Gong, H., Niu, G., Wang, F. “High Sensitivity Gas Sensor Based on Porous GaN Nanorods with Excellent High-Temperature Stability.” 20th International Conference on Solid-State Sensors, Actuators and Microsystems 1369-1372, (2019).

[55] Zhang, M., Zhao, C., Gong, H., Niu, G., Wang, F. “Porous GaN Submicron Rods for Gas Sensor with High Sensitivity and Excellent Stability at High Temperature.” ACS Applied Materials 11-33124-33131, (2019).

[56] Reddeppa, M., Park, B. G., Chinh, N. D., Kim, D., Oh, J. E., Kim, T. G., Kim, M. D. “A novel low-temperature resistive NO gas sensor based on InGaN/GaN multi-quantum well-embedded p-i-n GaN nanorods.” Dalton Transactions 48-1367-1375, (2019).

[57] Chandran, B., Janakiraman, K. "New Disposable Nitric Oxide Sensor Fabrication Using GaN Nanowires." ACS Omega 4-17171-17176, (2019).

[58] Khan, M. A. H., Thomson, B., Debnath, R., Rani, A., Motayed, A., Rao, M. V. "Reliable anatase-titania nanoclusters functionalized GaN sensor devices for UV assisted NO_2 gas-sensing in ppb level." Nanotechnology 31-155504, (2020).

[59] Shi, C., Rani, A., Thomson, B., Debnath, R., Motayed, A., Yoannou, D. E., Li, Q. "High-performance room-temperature TiO_2-functionalized GaN nanowire gas sensors." Applied Physics Letters 115-121602, (2019).

[60] Khan, M. A. H., Thomson, B., Yu, J., Debnath, R., Motayed, A., Rao, M. V. "Scalable metal oxide functionalized GaN nanowire for precise SO_2 detection." Sensors and Actuators B: Chemical-ScienceDirect 318-128223, (2020).

[61] Thomson, B., Shi, C., Rani, A., Debnath, R. M. "A. Low- power, Chip-Scale, Carbon Dioxide Gas Sensors for Spacesuit Monitoring." IEEE Sensors, P.6, (2018).

[62] Khan, M. A. H., Thomson, B., Debnath, R., Motayed, A., Rao, M. V. "Nanowire-Based Sensor Array for Detection of Cross-Sensitive Gases Using PCA and Machine Learning Algorithms." IEEE Sensors 20-6020-6028, (2020).

[63] Khan, M. A. H., Motayed, A., Rao, M. V. "Identification and Quantification of Gases and Their Mixtures Using GaN Sensor Array and Artificial Neural Network." Measurement Science and Technology, ECS J. (2020).

[64] Dong, Y., Dong-Hyeok, S., Quan, D., Jun-Hyeok, L., Chul-Ho, W., Jeong-Gil, K., Dunjun, C., Jung-Hee, L., Hai, L., Rong, Z., Youdou, Z. "High Sensitive pH Sensor Based on AlInN/GaN Heterostructure Transistor" Sensors, 18-1314, (2018).

© The Author(s) 2023. This article is an open access article distributed under the terms and conditions of the Creative Commons Attribution (CC BY) license (http://creativecommons.org/licenses/by/4.0/).